AFRL-RY-HS-TR-2011-00781

An Approach to Minimizing Probe Array/Target Interactions for Near Field Scattering Measurements

John K. Schindler

Solid State Scientific Corporation
Hollis, NH 03409

13 May 2011

Interim Report

AIR FORCE RESEARCH LABORATORY
Sensors Directorate
Electromagnetics Technology Division
80 Scott Drive
Hanscom AFB MA 01731-2909

NOTICE AND SIGNATURE PAGE

Distribution: Unlimited, Statement A

NOTICE

USING GOVERNMENT DRAWINGS, SPECIFICATIONS, OR OTHER DATA INCLUDED IN THIS DOCUMENT FOR ANY PURPOSE OTHER THAN GOVERNMENT PROCUREMENT DOES NOT IN ANY WAY OBLIGATE THE US GOVERNMENT. THE FACT THAT THE GOVERNMENT FORMULATED OR SUPPLIED THE DRAWINGS, SPECIFICATIONS, OR OTHER DATA DOES NOT LICENSE THE HOLDER OR ANY OTHER PERSON OR CORPORATION; OR CONVEY ANY RIGHTS OR PERMISSION TO MANUFACTURE, USE, OR SELL ANY PATENTED INVENTION THAT MAY RELATE TO THEM.

THIS TECHNICAL REPORT WAS CLEARED FOR PUBLIC RELEASE BY THE ELECTRONICS SYSTEMS CENTER PUBLIC AFFAIRS OFFICE FOR THE AIR FORCE RESEARCH LABORATORY ELECTROMAGNETICS TECHNOLOGY DIVISION AND IS AVAILABLE TO THE GENERAL PUBLIC, INCLUDING FOREIGN NATIONALS. COPIES MAY BE OBTAINED FROM THE DEFENSE TECHNICAL INFROMATION CENTER (DTIC) (http://www.dtic.mil)

AFRL-RY-HS-TR-2011-0781 HAS BEEN REVIEWED AND IS APPROVED FOR PUBLICATION IN ACCORDANCE WITH ASSIGNED DISTRIBUTION STATEMENT.

KRISTOPHER T. KIM
Research Physicist
Electromagnetic Scattering Branch

BERTUS WEIJERS
Branch Chief
Electromagnetic Scattering Branch

ROBERT V. McGAHAN
Technical Communication Advisor
Electromagnetics Technology Division

This report is published in the interest of scientific and technical information exchange and does not constitute the Government's approval or disapproval of its ideas or findings.

REPORT DOCUMENTATION PAGE

Form Approved
OMB No. 0704-0188

PLEASE DO NOT RETURN YOUR FORM TO THE ABOVE ADDRESS.

1. REPORT DATE *(DD-MM-YYYY)*	2. REPORT TYPE	3. DATES COVERED *(From - To)*
13-05-2011	INTERIM IN-HOUSE REPORT	1 OCT 2010 - 13 MAY 2011

4. TITLE AND SUBTITLE

An Approach to Minimizing Probe Array/Target Interactions for Near Field Scattering Measurements

5a. CONTRACT NUMBER
N/A

5b. GRANT NUMBER
N/A

5c. PROGRAM ELEMENT NUMBER
61102F

6. AUTHOR(S)
John K. Schindler, Solid State Scientific Corporation, Nashua, NH

5d. PROJECT NUMBER
2307

5e. TASK NUMBER
HE

5f. WORK UNIT NUMBER
01

7. PERFORMING ORGANIZATION NAME(S) AND ADDRESS(ES)
AFRL/RYHE, 80 Scott Drive, Hanscom AFB, MA 01731-2909
Solid State Scientific Corporation, 27-2 Wright Road, Hollis NH 03049

8. PERFORMING ORGANIZATION REPORT NUMBER
N/A

9. SPONSORING/MONITORING AGENCY NAME(S) AND ADDRESS(ES)
Electromagnetics Technology Division SC: 437490
Sensors Directorate
Air Force Research Laboratory
80 Scott Drive Hanscom AFB, MA 01731-2909

10. SPONSOR/MONITOR'S ACRONYM(S)
AFRL-RY-HS

11. SPONSOR/MONITOR'S REPORT NUMBER(S)
AFRL-RY-HS-TR-2011-0781

12. DISTRIBUTION/AVAILABILITY STATEMENT
Approved for public release; distribution unlimited. ESC PA 66ABW-2011-0781

13. SUPPLEMENTARY NOTES

14. ABSTRACT

We describe an effort to reduce the time required for near field scattering measurements by using an array of near field probes to replace the single probe that is conventionally used. An array of near field probes introduces technical problems. Coupling between the array and the scattering body may introduce errors in the near field measurements by perturbing the plane wave induced currents on the body. Mutual coupling between the probe array elements in the presence of the scattering body may change the near field measured at each probe array element. We analyze these technical problems and describe an approach to compensate for the errors introduced by the use of the probe array. Using an impedance model for the interactions between the probe array and the scattering body, we develop expressions for the measured voltages at each of the transmission line feeds to the probe array elements in terms of (1) the open circuit voltages induced by the plane wave excited body and (2) the in situ mutual impedances of the probe array. The expressions show a linear set of relations to the open circuit voltages.

15. SUBJECT TERMS

Bistatic Radar Cross Section, Near Field Scattering Measurements, Array Antennas

16. SECURITY CLASSIFICATION OF:			17. LIMITATION OF ABSTRACT	18. NUMBER OF PAGES	19a. NAME OF RESPONSIBLE PERSON
a. REPORT	b. ABSTRACT	c. THIS PAGE			Kristopher T. Kim
U	U	U	UU	27	19b. TELEPHONE NUMBER *(Include area code)*

Reset

Standard Form 298 (Rev. 8/98)
Prescribed by ANSI Std. Z39.18

Contents

List of Figures

1 Summary

Accurate estimation of the bistatic radar cross section of large vehicles is important for the design of advanced radar systems that employ spatially-distributed transmitters and receivers. These advanced systems can enhance radar performance through the use of multiple input/multiple output (MIMO) operation while reducing the vulnerability to countermeasures such as jamming and anti-radiation weapons. However, the measurement of bistatic radar cross sections of large vehicles with far-field techniques can be time consuming, expensive, and requires physically large and less secure measurement facilities. The measurements must be made over a large set of angles, frequencies, and polarizations for each orientation of the vehicle with respect to potential transmit sources. Alternatively, near-field scattering measurements permit estimation of bistatic scattering using smaller and more secure facilities. The use of advanced, electromagnetic processing enables the transformation of the multiple, near-field measurements to the required complete set of far-field cross sections. Still, near-field measurements are time consuming and therefore expensive. The objective of this work is to investigate the feasibility of significantly reducing the time to make near-field scattering measurements through the use of an array of near-field probes instead of the conventional single probe.

The use of an array of near-field probes introduces technical problems. Coupling between the probe array and the scattering body may introduce errors in the near-field measurements. Currents induced on the probe array and its support structure will reradiate and change the plane wave-induced currents on the scattering body. Further, mutual coupling between the probe array elements in the presence of the scattering body may change the near field measured at each probe array element from that measured by an isolated probe. In this work, we analyze these technical problems and describe an approach to compensate for the errors introduced by the use of the probe array.

Based on an impedance model for the interactions between the probe array and the scattering body, we have developed expressions for the measured voltages at each of the transmission line feeds to the probe array elements in terms of (1) the open-circuit voltages induced by the plane wave-excited body at each probe array element and (2) the in situ mutual impedances of the probe array. The expressions show a linear set of relations to the open-circuit voltages as would be expected by the superposition principle applied to this linear system. The linear set of equations can be inverted to yield the open-circuit, plane wave-induced voltages at each probe array element. We hypothesize that these voltages, when corrected for the direct plane wave excitation, are linearly related to the required near-field measurements. We also describe a separate set of vector network analyzer measurements to yield the in situ mutual impedances (the mutual impedances in the presence of the scattering body) that are required to invert the measurement equations.

Simple examples of the importance of the open-circuit conditions in the measurement of near fields with a dipole probe array are given. The results shown in the examples are based on a method of moments solution to the electromagnetic interaction problem using NEC4. In these examples the scattering target is considered to be an array of half-wavelength dipoles both near and far from the probe array. The target dipoles are a convenient surrogate for a more complex

target since perturbations in the induced currents due to the presence of the probe array are easily found. The open-circuit conditions for the elements of the probe array minimize the dominant currents on the elements leaving smaller, residual currents on the remaining quarter-wavelength sections of the dipoles. Minimization of the dominant currents in the probe array elements reduces the errors in the target dipole currents by more than 20 dB when compared to the free space-induced currents.

The preliminary results shown here are encouraging and suggest further analysis of open issues. These issues include (1) calibration of the open-circuit, plane wave-induced voltages and their relationship to the required near-field measurements, (2) necessity and accuracy requirements for in situ near-field impedance measurements to characterize the probe array as its positions changes with respect to the scattering body, and (3) experimental and/or numerical confirmation of the theory described in this report.

2 Introduction

As part of a program to advance the art of bistatic radar cross section measurements, we consider the use of an array of field probes to facilitate simultaneous, near-field measurements of the electromagnetic scattering from which bistatic cross sections are estimated. A significant number of near-field measurements are required for bistatic cross section determination and the use of an array of measurement probes will substantially reduce the time for bistatic cross section characterization. However, the electromagnetic interaction between an array of measurement probes and the scattering body may be significant enough to modify the plane wave-induced current distribution on the scattering body to be measured, thus causing errors in the estimated bistatic cross sections. The objective of this note is to investigate an approach to minimize the interaction between the array probe elements and the nearby scattering body.

Specifically, we consider an array of dipole field probes located near a scattering body when the body is illuminated by a plane wave source. Both the plane wave source and the body induce currents in the dipole field probes which, in turn, reradiate to the scattering body. Since the field probes are located near the scattering body, we expect that the probe reradiated fields will disturb the currents on the scattering body as induced by the plane wave excitation, causing errors in the scattered field measurements. Further, the field samples at each probe are influenced by the mutual coupling to other elements in the probe array, thus introducing errors in the field samples. The mutual coupling between elements of the probe array depends on the orientation of the array with respect to the scattering body and are likely to change as the array orientation with respect to the scattering body changes.

In this work we investigate the following basic questions:

- Is it possible to reduce the errors in probe field samples caused by mutual coupling between the array elements?
- Is it possible to minimize the scattering from the probe array in the near-field volume occupied by the scattering body?

In response to the second question, we analyze an approach to minimizing the dominant mode currents in the dipole elements of the probe array, thus minimizing the reradiation to the scattering body. In the process of minimizing the dominant mode currents, the effects of the in situ mutual coupling between array elements must be considered, in effect resolving the issue raised in the first question.

3 Model for the Probe Array Located in the Scatterer Environment

We begin by viewing the near-field measurement system as a linear system characterized by mutual impedances between elements of the system [1] as illustrated in Figure 1. Here the plane wave source excites the scattering body and the measurement background which is characterized by an unknown collection of virtual scattering sources. The plane wave source also excites the measurement array consisting of a collection of field probes terminated in sources and/or load impedances. The mutual coupling between array elements is characterized by the in situ mutual impedance array, Z_A, giving the voltage induced in each probe array element by the currents in the other array elements when the array is in the presence of the scattering body. Note that we have made the tacit assumption that there is no coupling between the scattering body and the plane wave source and between the array and the plane wave source. This is because the scattering from the body and array is weak at the extended range of the plane wave source.

The details of the scattering source are unknown and change with the orientation of the scattering source with respect to the measurement array and the plane wave source. For that reason, we focus on characterizing the coupling between the plane wave source, Z_{PA}, and the coupling between array elements in the presence of the scattering source, Z_A.

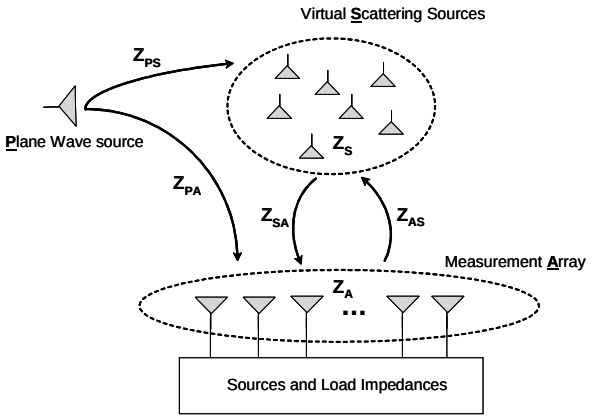

Figure 1: Impedance Characterization of Probe Array Measurement System

We characterizing the array-source-scatterer in terms of an $N + 2$-port linear network. Here there will be N array elements. One of the remaining ports is the source of plane wave excitation of the target and probe array and the other "port" is associated with a vector of ports associated with the natural mode currents on the scattering body.

For simplicity throughout this paper we will consider an $N = 3$ element array since the results for larger arrays will be an obvious extension. Then the impedance matrix characterizing the three element probe array measurement system is

$$\begin{bmatrix} E_p \\ \overline{E}_s \\ E_1 \\ E_2 \\ E_3 \end{bmatrix} = \begin{bmatrix} Z_{p,p} & \overline{Z}_{p,s}^T & Z_{p,1} & Z_{p,2} & Z_{p,3} \\ \overline{Z}_{s,p} & \overline{\overline{Z}}_{s,s} & \overline{Z}_{s,1} & \overline{Z}_{s,2} & \overline{Z}_{s,3} \\ Z_{1,p} & \overline{Z}_{1,s}^T & Z_{1,1} & Z_{1,2} & Z_{1,3} \\ Z_{2,p} & \overline{Z}_{2,s}^T & Z_{2,1} & Z_{2,2} & Z_{2,3} \\ Z_{3,p} & \overline{Z}_{3,s}^T & Z_{3,1} & Z_{3,2} & Z_{3,3} \end{bmatrix} \begin{bmatrix} I_p \\ \overline{I}_s \\ I_1 \\ I_2 \\ I_3 \end{bmatrix}. \tag{1}$$

Here E_p, $\overline{E}_s$ and E_i, $i = 1, 2, 3$ are the plane wave source, scattering body natural mode, and dipole voltages, respectively and I_p, $\overline{I}_s$, and I_i, $i = 1, 2, 3$ are the corresponding terminal currents. The impedances, $Z_{i,j}$, $i, j = 1, 2, 3$, are the mutual and self impedances of the array elements with the target present. The impedance matrix $\overline{\overline{Z}}_{s,s}$ characterizes the self and mutual impedances of the natural modes of the scattering body and the column matrix $\overline{Z}_{s,p}$ characterizes the coupling between the natural modes and the plane wave source. Finally, the impedance column matrices $\overline{Z}_{s,1}$, $\overline{Z}_{s,2}$, and $\overline{Z}_{s,3}$ characterized the coupling between the natural modes of the scattering body and the elements of the probe array.

We focus on the last three rows of this matrix characterizing the probe dipole voltages and currents and the open-circuit voltages induced in the dipole elements by the plane wave. That is,

$$\begin{bmatrix} E_1 \\ E_2 \\ E_3 \end{bmatrix} = \begin{bmatrix} Z_{1,p} \\ Z_{2,p} \\ Z_{3.p} \end{bmatrix} I_p + \begin{bmatrix} \overline{Z}_{1,s}^T \\ \overline{Z}_{2,s}^T \\ \overline{Z}_{3,s}^T \end{bmatrix} \overline{I}_s + \begin{bmatrix} Z_{1,1} & Z_{1,2} & Z_{1,3} \\ Z_{2,1} & Z_{2,2} & Z_{2,3} \\ Z_{3,1} & Z_{3,2} & Z_{3,3} \end{bmatrix} \begin{bmatrix} I_1 \\ I_2 \\ I_3 \end{bmatrix}. \tag{2}$$

Now the currents in the scatterer natural modes can be found from the second row equation of (1) by assuming that the scatterer terminals are loaded with equivalent impedances $\overline{\overline{Z}}_s$ giving

$$-\overline{\overline{Z}}_s \overline{I}_s = \overline{Z}_{s,p} I_p + \overline{\overline{Z}}_{s,s} \overline{I}_s + \overline{Z}_{s,1} I_1 + \overline{Z}_{s,2} I_2 + \overline{Z}_{s,3} I_3,$$

or

$$\overline{I}_s = -(\overline{\overline{Z}}_{s,s} + \overline{\overline{Z}}_s)^{-1} \overline{Z}_{s,p} I_p - (\overline{\overline{Z}}_{s,s} + \overline{\overline{Z}}_s)^{-1} \overline{Z}_{s,1} I_1 - (\overline{\overline{Z}}_{s,s} + \overline{\overline{Z}}_s)^{-1} \overline{Z}_{s,2} I_2 - (\overline{\overline{Z}}_{s,s} + \overline{\overline{Z}}_s)^{-1} \overline{Z}_{s,3} I_3.$$

Substituting into Equation 2 gives

$$\begin{bmatrix} E_1 \\ E_2 \\ E_3 \end{bmatrix} = \begin{bmatrix} E_1^P \\ E_2^P \\ E_3^P \end{bmatrix} + \begin{bmatrix} \widetilde{Z}_{1,1} & \widetilde{Z}_{1,2} & \widetilde{Z}_{1,3} \\ \widetilde{Z}_{2,1} & \widetilde{Z}_{2,2} & \widetilde{Z}_{2,3} \\ \widetilde{Z}_{3,1} & \widetilde{Z}_{3,2} & \widetilde{Z}_{3,3} \end{bmatrix} \begin{bmatrix} I_1 \\ I_2 \\ I_3 \end{bmatrix}, \tag{3}$$

where

$$\begin{aligned} E_i^P &= [Z_{i,p} - \overline{Z}_{i,s}^T (\overline{\overline{Z}}_{s,s} + \overline{\overline{Z}}_s)^{-1} \overline{Z}_{s,p}] I_p \quad && i = 1, 2, 3, \\ \widetilde{Z}_{i,i} &= Z_{i,i} - \overline{Z}_{i,,s}^T (\overline{\overline{Z}}_{s,s} + \overline{\overline{Z}}_s)^{-1} \overline{Z}_{s,i} && i = 1, 2, 3, \\ \widetilde{Z}_{i,j} &= Z_{i,j} && i \neq j. \end{aligned}$$

Here E_i^P, $i = 1, 2, 3$ represent the open-circuit voltages induced in each probe array element by the incident plane wave source in the presence of the scattering body and $\widetilde{Z}_{i,j}, i, j = 1, 2, 3$ are the in-situ mutual impedances of the probe array. In neglecting consideration of the first equation we have assumed that any radiation from the dipole elements in the presence of the scattering body and the scattering from the body itself does not change the primary source of plane wave excitation, as noted earlier.

It is important to note that each of the the plane wave-induced, open-circuit voltages, E_i^P, is the superposition of (1) a voltage due to the direct excitation of the probe array element by the plane wave, $Z_{i,p}I_p$, and (2) a voltage due to the scattering from the body when excited by the plane wave, $\overline{Z}_{i,s}^T(\overline{\overline{Z}}_{s,s} + \overline{\overline{Z}}_s)^{-1}\overline{Z}_{s,p}I_p$. In this report, we will develop an approach to measuring the open-circuit voltages, E_i^P, which, when corrected by removing the direct excitation term, are proportional to the near-zone scattered fields at the probe array elements.

Equation 3 suggests the N-port representation of the probe array measurement system as illustrated in Figure 2. Here the ports are the probe array element terminals with voltages E_i and currents $I_i, i = 1, 2, \ldots, N$. Each port has the open-circuit voltage, E_i^P, induced by the plane wave source in the presence of the scattering body.

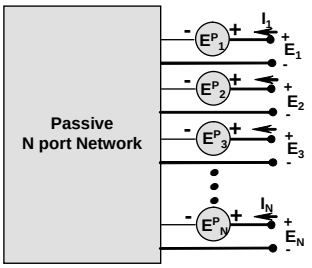

Figure 2: N-Port Equivalent Circuit of Measurement System

4 Minimizing Probe Array Interactions

We develop an approach to actively load the terminals of the probe array to minimize array reradiation which can modify the plane wave induced currents on the scattering body. In the following sections we develop a theoretical basis for minimizing the currents in the probe array elements and present an elementary example to demonstrate performance.

4.1 Basic Theory

The objective in this work is to actively load the terminals of the probe array to minimize array reradiation which can modify the plane wave currents on the scattering body. To that end we

consider the model for the N-port measurement system with Thévenin equivalent source voltages E_{si} and impedances Z_{si}, $i = 1, 2, \ldots, N$ at the probe array terminals as shown in Figure 3.

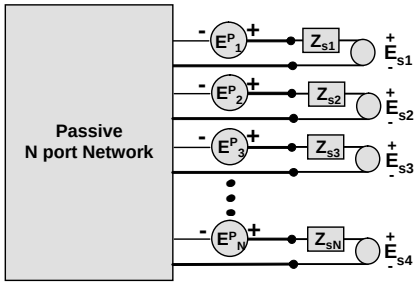

Figure 3: N-Port Measurement System with Thévenin Equivalent Sources at each Terminal

In this case, the simplified network equations given by Equation (3) become

$$\begin{bmatrix} E_1 \\ E_2 \\ E_3 \end{bmatrix} = \begin{bmatrix} E_{s1} - Z_{s1} I_1 \\ E_{s2} - Z_{s2} I_2 \\ E_{s3} - Z_{s3} I_3 \end{bmatrix} = \begin{bmatrix} E_1^P \\ E_2^P \\ E_3^P \end{bmatrix} + \begin{bmatrix} \widetilde{Z}_{1,1} & \widetilde{Z}_{1,2} & \widetilde{Z}_{1,3} \\ \widetilde{Z}_{2,1} & \widetilde{Z}_{2,2} & \widetilde{Z}_{2,3} \\ \widetilde{Z}_{3,1} & \widetilde{Z}_{3,2} & \widetilde{Z}_{3,3} \end{bmatrix} \begin{bmatrix} I_1 \\ I_2 \\ I_3 \end{bmatrix},$$

which is equivalent to

$$\begin{bmatrix} E_{s1} - E_1^P \\ E_{s2} - E_2^P \\ E_{s3} - E_3^P \end{bmatrix} = \begin{bmatrix} \widetilde{Z}_{1,1} + Z_{s1} & \widetilde{Z}_{1,2} & \widetilde{Z}_{1,3} \\ \widetilde{Z}_{2,1} & \widetilde{Z}_{2,2} + Z_{s2} & \widetilde{Z}_{2,3} \\ \widetilde{Z}_{3,1} & \widetilde{Z}_{3,2} & \widetilde{Z}_{3,3} + Z_{s3} \end{bmatrix} \begin{bmatrix} I_1 \\ I_2 \\ I_3 \end{bmatrix}. \tag{4}$$

It is clear from these equations that forcing all elements of the column matrix on the left side to be equal to zero assures that the currents induced in each probe element port will be zero, providing of course that the augmented impedance matrix is not singular. Requiring that the column matrix to the left be zero is equivalent to requiring that the open-circuit Thévenin equivalent source voltage at each port be equal to the open-circuit voltage in each probe array element induced by the plane wave excitation in the presence of the scattering body.

4.2 Elementary Example

To illustrate this point we consider the following elementary numerical example. Here a single measurement dipole is located near a collection of passive, target dipoles which serve to represent the measurement body. The measurement dipole and target dipoles are illuminated by a plane wave. The use of dipoles is both convenient and practical. The electromagnetic environment will be characterized by the Numerical Electromagnetic Code (NEC4) which conveniently determines the interaction between collections of dipoles which may be loaded and excited by local sources as well as a plane wave source. Further, the dipole is a practical measurement probe used in some antenna and cross section ranges. Also, dipoles are a convenient surrogate for the scattering body since, with the NEC code, perturbations of the currents on the scattering dipoles can be determined as a measure of the magnitude of the probe-scatterer interactions. In this example,

the measurement dipole will be fed by a source at its center. We will determine the required source voltage to cancel the induced current on the measurement dipole and then examine the current perturbations on the scattering dipoles.

Specifically, the single measurement probe consists of a thin dipole of length 0.48λ, where λ denotes the free-space wavelength of the measurement plane wave. The probe dipole can be excited by a voltage source at its center. The voltage source is assumed to be coherent with respect to the plane-wave illumination. That is, the frequency of the voltage source is that of the plane wave and its phase is constant during measurements. As illustrated in Figure 4, two target dipoles are located adjacent to the measurement probe. Both are half-wavelength dipoles. One is located 5λ from the probe and the other is located at 35λ away from the probe and offset by 5λ. The collection of probe-target dipoles is excited by a plane wave with an E field strength of 1v/m.

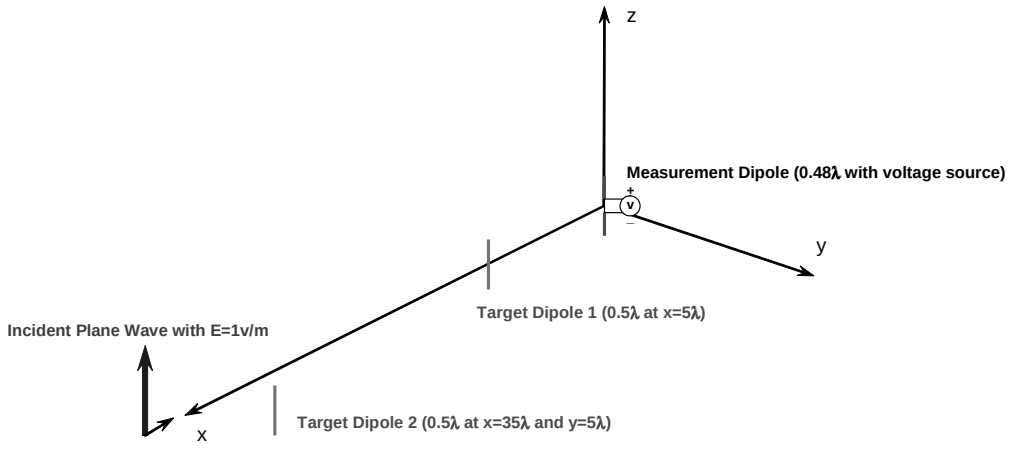

Figure 4: Geometry for Simple Example of Single Probe Element and Target Dipoles

We use NEC4 to determine relevant properties of the probe and target dipole current distributions. First, we determine the short-circuit current due to plane wave excitation at the center of the probe dipole when the target dipoles are present. This is done by requiring that the probe dipole voltage source be zero volts. Second, we determine the current excited by the voltage source at the center of the probe dipole when the target dipoles are present and there is no plane-wave excitation. Finally, using superposition in this linear system with both plane wave and voltage source excitations, the voltage is adjusted to create a current that cancels that induced by the plane wave. The effectiveness of the cancelation is determined by comparing the currents in the target dipoles with those induced in the dipoles when the probe is removed.

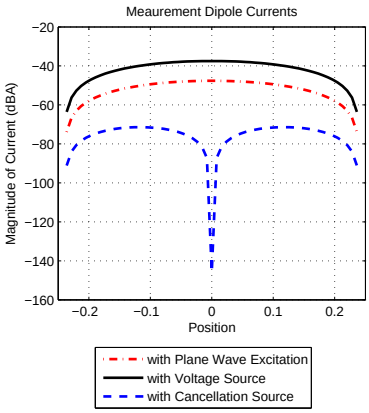

Figure 5: Current Distributions on Measurement Dipole in Simple Example

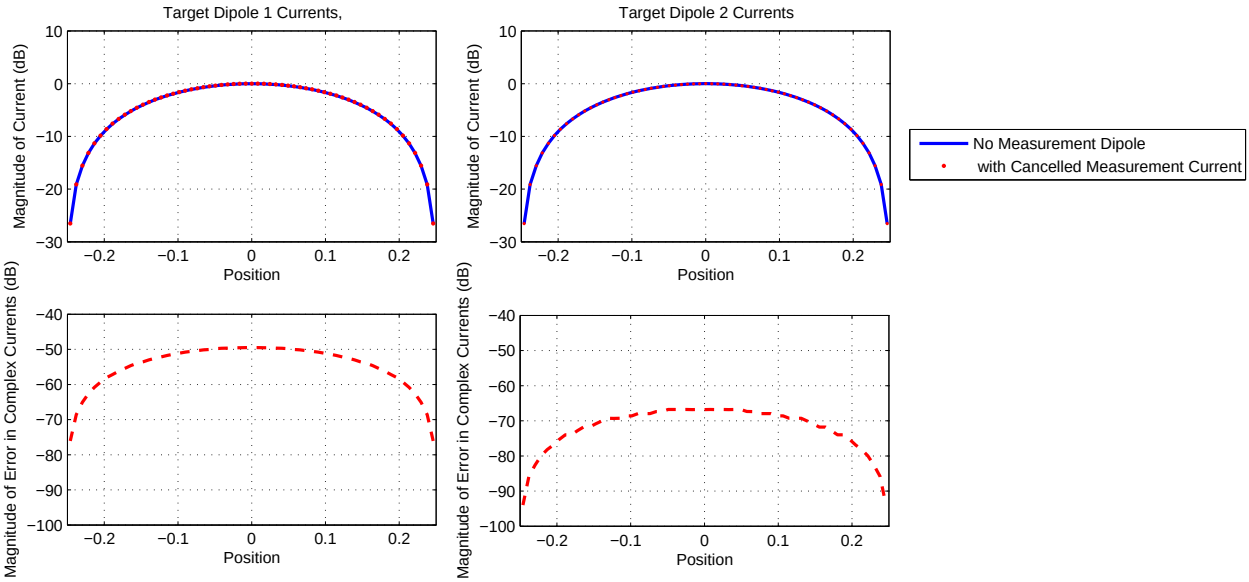

Figure 6: Current Distributions in Target Dipoles and Current Errors Due to Presence of Measurement Dipole with Canceled Current

Figures 5 and 6 show the results. Figure 5 shows the measurement dipole currents with plane wave, voltage, and cancelation sources. The voltage source is set at 1 volt. Note that the current is effectively canceled at the center of the measurement dipole where the cancelation voltage is applied. However, a residual current remains which is approximately 10 dB below the current induced by the incident plane wave. While this does not appear to be a substantial cancelation of the measurement dipole current, the real measure of effectiveness is the perturbation in currents induced in the target dipoles. These results are shown in Figure 6.

The target dipole currents with no measurement dipole present and with the canceled current on the measurement dipole are shown in the upper row. Since the difference between the currents is

too small to note in these graphs, plots of the magnitude of the error in the complex currents are presented in the second row. For the near dipole (5λ away from the measurement dipole), the error is less than -50 dB below the magnitude of the current on the dipole. For the distant dipole (35λ away from the measurement dipole), the error is less than -65 dB below the target dipole current magnitude.

We conclude that even a modest reduction in the measurement dipole currents results in very small errors in the target dipole currents when compared to currents induced in the free-space environment alone. This is an encouraging illustration of the approach described here and forms the basis for the following analysis of a more realistic measurement system.

4.3 Open-Circuit Induced Voltages on Probe Array Elements

It is clear from the previous discussion of Equation 4 that the plane wave-induced open-circuit voltage at each terminal of the probe array must be measured. In the following we suggest an approach to making those measurements.

We begin by adopting a more realistic model for the N-port network representing the measurement array (Figure 3) where now each network terminal is connected to its Thévenin equivalent source through a transmission line. This model is shown in Figure 7. To understand the process by which we measure the plane wave-induced open-circuit voltages, we develop the Thévenin equivalent circuit for the N-port probe array network at each network port with the transmission lines and loads at the other ports. This is illustrated in Figure 8 where the arrow indicates the point at which the Thévenin equivalent circuit is to be developed at network terminal 1 and the other transmission lines are shown loaded by their Thévenin equivalent source impedances.

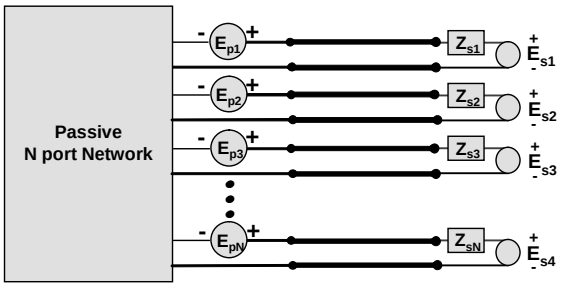

Figure 7: N-Port Equivalent Circuit of Measurement System with Transmission Line and Sources at Each Port

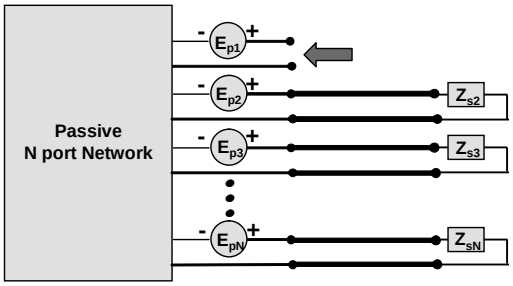

Figure 8: N-Port Equivalent Circuit for Finding Thévenin Equivalent Circuit

We develop the network equivalent circuit at port 1 assuming a three-port network. From Equation (3) we can write the following equations which determine the equivalent open-circuit voltage, E_1^{oc}, of the Thévenin equivalent circuit

$$\begin{bmatrix} E_1 \\ E_2 \\ E_3 \end{bmatrix} = \begin{bmatrix} E_1^{oc} \\ -Z_2 I_2 \\ -Z_3 I_3 \end{bmatrix} = \begin{bmatrix} E_1^P \\ E_2^P \\ E_3^P \end{bmatrix} + \begin{bmatrix} \widetilde{Z}_{1,1} & \widetilde{Z}_{1,2} & \widetilde{Z}_{1,3} \\ \widetilde{Z}_{2,1} & \widetilde{Z}_{2,2} & \widetilde{Z}_{2,3} \\ \widetilde{Z}_{3,1} & \widetilde{Z}_{3,2} & \widetilde{Z}_{3,3} \end{bmatrix} \begin{bmatrix} 0 \\ I_2 \\ I_3 \end{bmatrix},$$

where by setting $I_1 = 0$ we find the open-circuit voltage at port 1. Note that the other network ports are loaded with impedances Z_2 and Z_3 and the negative signs account for the convention that the port currents are assumed to be positive when they enter the port terminal. The load impedances are easily found from the transmission line equations [1] at each port as

$$Z_i = Z_o \frac{1 + \Gamma_i e^{-j2kL_i}}{1 - \Gamma_i e^{-j2kL_i}}, \tag{5}$$

where

$$\Gamma_i = \frac{Z_{si} - Z_o}{Z_{si} + Z_o},$$

and $Z_o =$ the characteristic impedance of the transmission line, $L_i =$ the length of the transmission line at port i and $k = 2\pi/\lambda$.

It follows from the first of the set of equations that

$$\begin{aligned} E_1^{oc} &= E_1^P + \begin{bmatrix} \widetilde{Z}_{1,2} & \widetilde{Z}_{1,3} \end{bmatrix} \begin{bmatrix} I_2 \\ I_3 \end{bmatrix} \\ &= E_1^P - \begin{bmatrix} \widetilde{Z}_{1,2} & \widetilde{Z}_{1,3} \end{bmatrix} \begin{bmatrix} \widetilde{Z}_{2,2} + Z_2 & \widetilde{Z}_{2,3} \\ \widetilde{Z}_{3,2} & \widetilde{Z}_{3,3} + Z_3 \end{bmatrix}^{-1} \begin{bmatrix} E_2^P \\ E_3^P \end{bmatrix}. \end{aligned} \tag{6}$$

Here the second and third of the set of equations have been solved for the currents I_2 and I_3 and substituted into the first equation.

To develop the Thévenin equivalent impedance, we determine the short-circuit current at port 1, I_1^{sc}, since the Thévenin equivalent impedance is the ratio $Z_{1Th} = E_1^{oc}/I_1^{sc}$. Again, referring to Equation 3 we can write

$$\begin{bmatrix} E_1 \\ E_2 \\ E_3 \end{bmatrix} = \begin{bmatrix} 0 \\ -Z_2 I_2 \\ -Z_3 I_3 \end{bmatrix} = \begin{bmatrix} E_1^P \\ E_2^P \\ E_3^P \end{bmatrix} + \begin{bmatrix} \widetilde{Z}_{1,1} & \widetilde{Z}_{1,2} & \widetilde{Z}_{1,3} \\ \widetilde{Z}_{2,1} & \widetilde{Z}_{2,2} & \widetilde{Z}_{2,3} \\ \widetilde{Z}_{3,1} & \widetilde{Z}_{3,2} & \widetilde{Z}_{3,3} \end{bmatrix} \begin{bmatrix} -I_1^{sc} \\ I_2 \\ I_3 \end{bmatrix}.$$

The short-circuit current at port 1 is determined from the first of the set of equations by requiring that $E_1 = 0$. Note that the current $I_1 = -I_1^{sc}$ where the minus sign is included to maintain the current convention for the Thévenin equivalent circuit. From the second and third of these equations we find

$$\begin{bmatrix} \widetilde{Z}_{2,1} \\ \widetilde{Z}_{3,1} \end{bmatrix} I_1^{sc} = \begin{bmatrix} E_2^P \\ E_3^P \end{bmatrix} + \begin{bmatrix} \widetilde{Z}_{2,2} + Z_2 & \widetilde{Z}_{2,3} \\ \widetilde{Z}_{3,2} & \widetilde{Z}_{3,3} + Z_3 \end{bmatrix} \begin{bmatrix} I_2 \\ I_3 \end{bmatrix}$$

Then from the first equation we find

$$\begin{aligned} E_1^P &= \widetilde{Z}_{1,1} I_1^{sc} - \begin{bmatrix} \widetilde{Z}_{1,2} & \widetilde{Z}_{1,3} \end{bmatrix} \begin{bmatrix} I_2 \\ I_3 \end{bmatrix} \\ &= \widetilde{Z}_{1,1} I_1^{sc} - \begin{bmatrix} \widetilde{Z}_{1,2} & \widetilde{Z}_{1,3} \end{bmatrix} \begin{bmatrix} \widetilde{Z}_{2,2} + Z_2 & \widetilde{Z}_{2,3} \\ \widetilde{Z}_{3,2} & \widetilde{Z}_{3,3} + Z_3 \end{bmatrix}^{-1} \left(\begin{bmatrix} \widetilde{Z}_{2,1} \\ \widetilde{Z}_{3,1} \end{bmatrix} I_1^{sc} - \begin{bmatrix} E_2^P \\ E_3^P \end{bmatrix} \right) \\ &= \left(\widetilde{Z}_{1,1} - \begin{bmatrix} \widetilde{Z}_{1,2} & \widetilde{Z}_{1,3} \end{bmatrix} \begin{bmatrix} \widetilde{Z}_{2,2} + Z_2 & \widetilde{Z}_{2,3} \\ \widetilde{Z}_{3,2} & \widetilde{Z}_{3,3} + Z_3 \end{bmatrix}^{-1} \begin{bmatrix} \widetilde{Z}_{2,1} \\ \widetilde{Z}_{3,1} \end{bmatrix} \right) I_1^{sc} \\ &\quad + \begin{bmatrix} \widetilde{Z}_{1,2} & \widetilde{Z}_{1,3} \end{bmatrix} \begin{bmatrix} \widetilde{Z}_{2,2} + Z_2 & \widetilde{Z}_{2,3} \\ \widetilde{Z}_{3,2} & \widetilde{Z}_{3,3} + Z_3 \end{bmatrix}^{-1} \begin{bmatrix} E_2^P \\ E_3^P \end{bmatrix}. \end{aligned}$$

Using the expression for E_1^{oc} in Equation 6, this result becomes

$$E_1^{oc} = \left(\widetilde{Z}_{1,1} - \begin{bmatrix} \widetilde{Z}_{1,2} & \widetilde{Z}_{1,3} \end{bmatrix} \begin{bmatrix} \widetilde{Z}_{2,2} + Z_2 & \widetilde{Z}_{2,3} \\ \widetilde{Z}_{3,2} & \widetilde{Z}_{3,3} + Z_3 \end{bmatrix}^{-1} \begin{bmatrix} \widetilde{Z}_{2,1} \\ \widetilde{Z}_{3,1} \end{bmatrix} \right) I_1^{sc},$$

where the Thévenin equivalent impedance at port 1 is

$$Z_{1Th} = E_1^{oc}/I_1^{sc} = \widetilde{Z}_{1,1} - \begin{bmatrix} \widetilde{Z}_{1,2} & \widetilde{Z}_{1,3} \end{bmatrix} \begin{bmatrix} \widetilde{Z}_{2,2} + Z_2 & \widetilde{Z}_{2,3} \\ \widetilde{Z}_{3,2} & \widetilde{Z}_{3,3} + Z_3 \end{bmatrix}^{-1} \begin{bmatrix} \widetilde{Z}_{2,1} \\ \widetilde{Z}_{3,1} \end{bmatrix}. \tag{7}$$

Note that the Thévenin equivalent circuit for the loaded N-port (Equations (5, 6, and 7) require that we know the in situ self and mutual impedances of the probe array as well as the plane wave induced open-circuit voltages at each of the probe array ports.

To complete the analysis we transform the Thévenin equivalent source through the transmission line at port 1 to the source end of the transmission line. Here we require that the source end of the transmission line be loaded with the source impedance Z_{s1} and we set the source voltage $E_{s1} = 0$ volts as illustrated in Figure 9. With standard transmission line analysis [2] we find that the measured voltage at the source end of the transmission line is

$$E_{1m} = \frac{E_1^{oc} Z_o (1 + \Gamma_1)}{(Z_{1Th} + Z_o)(1 - \Gamma_{Th}\Gamma_1 e^{-j2kL_1})} e^{-jkL_1},$$

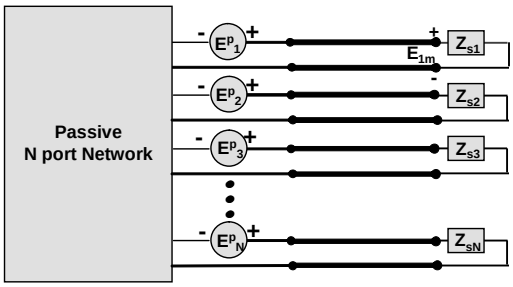

Figure 9: N-Port Equivalent Circuit with Measurement Load

where

$$\Gamma_{Th} = \frac{Z_{1Th} - Z_o}{Z_{1Th} + Z_o}.$$

Substituting for E_1^{oc} from Equation 6 gives the measured voltage at source port 1 as

$$\begin{aligned} E_{1m} &= \frac{Z_o(1+\Gamma_1)}{(Z_{1Th}+Z_o)(1-\Gamma_{Th}\Gamma_1 e^{-j2kL_1})} e^{-jkL_1} \left(E_1^P - \left[\begin{array}{cc} \widetilde{Z}_{1,2} & \widetilde{Z}_{1,3} \end{array} \right] \left[\begin{array}{cc} \widetilde{Z}_{2,2}+Z_2 & \widetilde{Z}_{2,3} \\ \widetilde{Z}_{3,2} & \widetilde{Z}_{3,3}+Z_3 \end{array} \right]^{-1} \left[\begin{array}{c} E_2^P \\ E_3^P \end{array} \right] \right) \\ &= \frac{Z_o(1+\Gamma_1)}{(Z_{1Th}+Z_o)(1-\Gamma_{Th}\Gamma_1 e^{-j2kL_1})} e^{-jkL_1} \left(E_1^P - \frac{\left[\begin{array}{cc} \widetilde{Z}_{1,2} & \widetilde{Z}_{1,3} \end{array} \right] \left[\begin{array}{cc} \widetilde{Z}_{3,3}+Z_3 & -\widetilde{Z}_{3,2} \\ -\widetilde{Z}_{2,3} & \widetilde{Z}_{2,2}+Z_2 \end{array} \right] \left[\begin{array}{c} E_2^P \\ E_3^P \end{array} \right]}{\Delta} \right) \\ &= \frac{Z_o(1+\Gamma_1)}{(Z_{1Th}+Z_o)(1-\Gamma_{Th}\Gamma_1 e^{-j2kL_1})} e^{-jkL_1} \left(E_1^P - \frac{\tilde{Z}_{12}(\tilde{Z}_{33}+Z_3)-\widetilde{Z}_{1,3}\widetilde{Z}_{2,3}}{\Delta} E_2^P - \frac{\widetilde{Z}_{1,3}(\widetilde{Z}_{2,2}+Z_2)-\widetilde{Z}_{1,2}\widetilde{Z}_{3,2}}{\Delta} E_3^P \right). \end{aligned} \tag{8}$$

In this equation, Δ denotes the determinant of the reduced impedance matrix:

$$\Delta = \left| \begin{array}{cc} \widetilde{Z}_{2,2}+Z_2 & \widetilde{Z}_{2,3} \\ \widetilde{Z}_{3,2} & \widetilde{Z}_{3,3}+Z_3 \end{array} \right|.$$

It is important to note in Equation 8 that the measured voltage at source port 1 is a linear combination of the open-circuit, plane wave induced voltages at the network ports. Of course this is to be expected given that the measurement system is linear and the measured response must then be a linear combination of the system excitation voltages. By extension, the measured voltages at the other measurement ports, E_{2m} and E_{3m}, are linear combinations of the same open-circuit, plane wave induced voltages. Thus, in the case of the three port system, we have three linear equations which can be inverted to give the three required plane wave induced voltages. Note however, that this inversion requires that we measure independently the in situ impedance matrix given in Equation 3 when the plane wave excitation is turned off. We will describe an approach to measuring these impedances later in this paper.

Before we leave this development, we determine the source voltage required to cancel the current at the probe network terminals when the probe array is excited by a plane wave. Consider Figure 10 where measurement port 1 is driven by an active source with equivalent Thévenin open-circuit voltage E_{s1} and impedance Z_{s1}. The probe array plane wave excitation is characterized by the induced open-circuit voltages E_i^P, $i = 1, 2, \ldots, N$.

If we transform the Thévenin equivalent source to the probe array network port 1, a new equivalent source is formed at the probe array port with the open-circuit voltage and equivalent impedance [3]

$$E_{1seq} = \frac{2E_{s1}Z_o e^{-jkL_1}}{(Z_{s1}+Z_o)(1-\Gamma_{1seq})},$$

and

$$Z_{1seq} = Z_o \frac{Z_{1s} + jZ_o tan(kL_1)}{Z_o + jZ_{1s} tan(kL_1)} = Z_o \frac{1+\Gamma_{1seq}}{1-\Gamma_{1seq}},$$

where $\Gamma_{1seq} = \Gamma_{1s} e^{-j2kL_1}$ and $\Gamma_{1s} = \frac{Z_{1s}-Z_o}{Z_{1s}+Z_o}$.

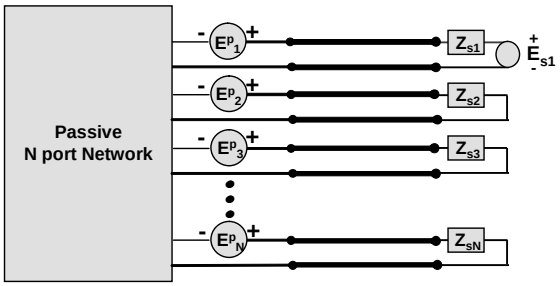

Figure 10: N-Port Equivalent Circuit with Active Load

Figure 11 illustrates the equivalent circuit at probe array port 1 where the equivalent circuit of the loaded probe array with plane wave illumination is shown to the left and the equivalent circuit for the source at measurement port 1 is shown to the right. It is clear from this illustration that to drive the port current to zero requires that $E_1^{oc} = E_{1seq}$ or

$$\frac{2E_{s1}Z_o e^{-jkL_1}}{(Z_{s1}+Z_o)(1-\Gamma_{1seq})} = E_1^P - \left[\begin{array}{cc} \widetilde{Z}_{1,2} & \widetilde{Z}_{1,3} \end{array}\right] \left[\begin{array}{cc} \widetilde{Z}_{2,2}+Z_2 & \widetilde{Z}_{2,3} \\ \widetilde{Z}_{3,2} & \widetilde{Z}_{3,3}+Z_3 \end{array}\right]^{-1} \left[\begin{array}{c} E_2^P \\ E_3^P \end{array}\right],$$

giving the required voltage a measurement port 1 as

$$E_{s1} = \frac{(Z_{s1}+Z_o)(1-\Gamma_{1seq})e^{jkL_1}}{2Z_o} \left[E_1^P - \left[\begin{array}{cc} \widetilde{Z}_{1,2} & \widetilde{Z}_{1,3} \end{array}\right] \left[\begin{array}{cc} \widetilde{Z}_{2,2}+Z_2 & \widetilde{Z}_{2,3} \\ \widetilde{Z}_{3,2} & \widetilde{Z}_{3,3}+Z_3 \end{array}\right]^{-1} \left[\begin{array}{c} E_2^P \\ E_3^P \end{array}\right]\right]. \quad (9)$$

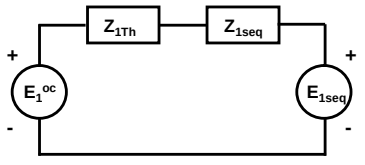

Figure 11: Load Voltage to Cancel Probe Current

Again we note that the cancelation voltage E_{s1} requires knowledge of not only the in situ self and mutual impedances of the probe array but also the plane wave induced open-circuit voltages at each of the probe array ports.

Recall that the objective of the probe array is the simultaneous measurement of the near-scattered field at each probe array element. It seems that the solution for the plane wave induced open-circuit voltages, E_i^P, $i = 1, 2, \ldots, N$, using Equation 8 and the measured voltages E_{im}, $i = 1, 2, \ldots, N$ would satisfy this objective, once the open-circuit voltages have been corrected for the term characterizing the direct plane wave excitation. Note that in this process we have determined the open-circuit voltages mathematically without physically inducing the zero current at each probe network port as implied in Equation 9.

4.4 Determination of Probe Array In Situ Impedances

Finally, we develop an approach to measure the in situ self and mutual impedances of the probe array which, as noted earlier, are required to determine the plane wave induced open-circuit probe array voltages. We adopt the basic measurement technique used in modern vector network analyzers. Consider the probe array network shown in Figure 12 with equivalent sources and transmission line feeds. We assume that there is no plane wave excitation for these measurements and that the source impedance matches the transmission line characteristic impedance, Z_o. The signals on each transmission line are characterized by their incident and reflected voltages, a_i^m and b_i^m, $i = 1, 2, \ldots, N$ respectively.

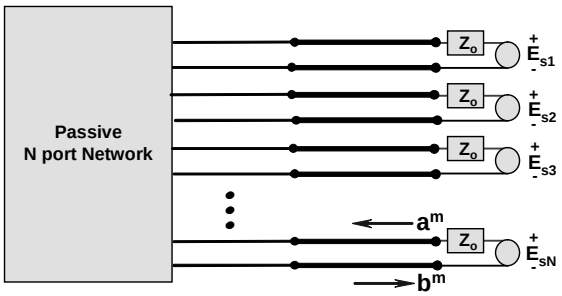

Figure 12: N-Port Equivalent Circuit for Finding Array Mutual and Self Impedances

The linear relationship between the incident and reflected voltages is characterized by the scattering matrix for the network and transmission lines as

$$\begin{bmatrix} b_1^m \\ b_2^m \\ b_3^m \end{bmatrix} = \begin{bmatrix} s_{11}^m & s_{12}^m & s_{13}^m \\ s_{21}^m & s_{22}^m & s_{23}^m \\ s_{31}^m & s_{32}^m & s_{33}^m \end{bmatrix} \begin{bmatrix} a_1^m \\ a_2^m \\ a_3^m \end{bmatrix}. \tag{10}$$

Here the superscript m denotes that these parameters refer to the measurement ports of the probe array network and transmission line system. Each of the scattering parameters can be determined from direct measurement of the incident and scattered voltages as, for example,

$$s_{23}^m = \frac{b_2^m}{a_3^m} \mid_{a_1^m = a_2^m = 0} .$$

The constraint $a_1^m = a_2^m = 0$ implies that the sources at measurement ports 1 and 2 are removed and all ports are terminated with the characteristic impedance of their transmission lines.

We require the scattering matrix and associated mutual impedance matrix for the probe array. To that end, we de-embed the incident and reflected voltages at the measurement ports to the probe array ports yielding a_i^a and b_i^a, $i = 1, 2, \ldots, N$. That is,

$$a_i^a = e^{-jkL_i} a_i^m \tag{11}$$

and

$$b_i^a = e^{jkL_i} b_i^m, \tag{12}$$

for all $i = 1, 2, \ldots, N$. Of course the incident and reflected voltages at the probe array ports yield the scattering matrix for the probe array as

$$\begin{bmatrix} b_1^a \\ b_2^a \\ b_3^a \end{bmatrix} = \begin{bmatrix} s_{11}^a & s_{12}^a & s_{13}^a \\ s_{21}^a & s_{22}^a & s_{23}^a \\ s_{31}^a & s_{32}^a & s_{33}^a \end{bmatrix} \begin{bmatrix} a_1^a \\ a_2^a \\ a_3^a \end{bmatrix}. \tag{13}$$

If we use Equations 11 and 12 with Equation 10 we can write

$$\begin{bmatrix} b_1^a \\ b_2^a \\ b_3^a \end{bmatrix} = \begin{bmatrix} e^{jkL_1} & 0 & 0 \\ 0 & e^{jkL_2} & 0 \\ 0 & 0 & e^{jkL_3} \end{bmatrix} \begin{bmatrix} b_1^m \\ b_2^m \\ b_3^m \end{bmatrix} = \begin{bmatrix} e^{jkL_1} & 0 & 0 \\ 0 & e^{jkL_2} & 0 \\ 0 & 0 & e^{jkL_3} \end{bmatrix} \begin{bmatrix} s_{11}^m & s_{12}^m & s_{13}^m \\ s_{21}^m & s_{22}^m & s_{23}^m \\ s_{31}^m & s_{32}^m & s_{33}^m \end{bmatrix} \begin{bmatrix} a_1^m \\ a_2^m \\ a_3^m \end{bmatrix}$$

$$= \begin{bmatrix} e^{jkL_1} & 0 & 0 \\ 0 & e^{jkL_2} & 0 \\ 0 & 0 & e^{jkL_3} \end{bmatrix} \begin{bmatrix} s_{11}^m & s_{12}^m & s_{13}^m \\ s_{21}^m & s_{22}^m & s_{23}^m \\ s_{31}^m & s_{32}^m & s_{33}^m \end{bmatrix} \begin{bmatrix} e^{jkL_1} & 0 & 0 \\ 0 & e^{jkL_2} & 0 \\ 0 & 0 & e^{jkL_3} \end{bmatrix} \begin{bmatrix} a_1^a \\ a_2^a \\ a_3^a \end{bmatrix},$$

providing an expression for the scattering matrix at the probe array ports in terms of the measured scattering matrix as

$$\begin{bmatrix} s_{11}^a & s_{12}^a & s_{13}^a \\ s_{21}^a & s_{22}^a & s_{23}^a \\ s_{31}^a & s_{32}^a & s_{33}^a \end{bmatrix} = \begin{bmatrix} e^{jkL_1} & 0 & 0 \\ 0 & e^{jkL_2} & 0 \\ 0 & 0 & e^{jkL_3} \end{bmatrix} \begin{bmatrix} s_{11}^m & s_{12}^m & s_{13}^m \\ s_{21}^m & s_{22}^m & s_{23}^m \\ s_{31}^m & s_{32}^m & s_{33}^m \end{bmatrix} \begin{bmatrix} e^{jkL_1} & 0 & 0 \\ 0 & e^{jkL_2} & 0 \\ 0 & 0 & e^{jkL_3} \end{bmatrix}$$

$$= \begin{bmatrix} s_{11}^m e^{j2kL_1} & s_{12}^m e^{jk(L_1+L_2)} & s_{13}^m e^{jk(L_1+L_3)} \\ s_{21}^m e^{jk(L_1+L_2)} & s_{22}^m e^{j2kL_2} & s_{23}^m e^{jk(L_2+L_3)} \\ s_{31}^m e^{jk(L_1+L_3)} & s_{32}^m e^{jk(L_2+L_3)} & s_{33}^m e^{j2kL_3} \end{bmatrix}. \tag{14}$$

Finally, we can convert the scattering matrix at the probe array ports to the array mutual impedance matrix. Recognizing that at each probe array port the transmission line voltages and currents are related to the incident and scattered wave complex amplitudes by

$$E_i^a = \sqrt{Z_o}(a_i^a + b_i^a)$$

and

$$I_i^a = \frac{1}{\sqrt{Z_o}}(a_i^a - b_i^a).$$

In matrix form

$$\overline{E}^a = \sqrt{Z_o}(\bar{a}^a + \bar{b}^a) = \bar{\bar{Z}}^a \overline{I}^a = \frac{\bar{\bar{Z}}^a}{\sqrt{Z_o}}(\bar{a}^a - \bar{b}^a).$$

This matrix equation can be solved for the probe array scattering matrix $\bar{\bar{S}}^a$ using the identity matrix $\overline{\overline{Id}}$ as

$$Z_o\overline{\overline{Id}}(\bar{a}^a + \bar{b}^a) = \bar{\bar{Z}}^a(\bar{a}^a - \bar{b}^a),$$

or

$$(\bar{\bar{Z}}^a + Z_o\overline{\overline{Id}})\bar{b}^a = (\bar{\bar{Z}}^a - Z_o\overline{\overline{Id}})\bar{a}^a,$$

so that the scattering matrix $\bar{\bar{S}}^a$ is given in terms of the array mutual impedance matrix by

$$\bar{b}^a = \bar{\bar{S}}^a\bar{a}^a = (\bar{\bar{Z}}^a + Z_o\overline{\overline{Id}})^{-1}(\bar{\bar{Z}}^a - Z_o\overline{\overline{Id}})\bar{a}^a.$$

This result can be inverted to yield the probe array mutual impedance matrix as follows:

$$\bar{\bar{S}}^a = (\bar{\bar{Z}}^a + Z_o\overline{\overline{Id}})^{-1}(\bar{\bar{Z}}^a - Z_o\overline{\overline{Id}})$$

or

$$(\bar{\bar{Z}}^a + Z_o\overline{\overline{Id}})\bar{\bar{S}}^a = (\bar{\bar{Z}}^a - Z_o\overline{\overline{Id}})$$

giving

$$\bar{\bar{Z}}^a(\overline{\overline{Id}} - \bar{\bar{S}}^a) = Z_o(\overline{\overline{Id}} + \bar{\bar{S}}^a)$$

so that

$$\bar{\bar{Z}}^a = Z_o(\overline{\overline{Id}} - \bar{\bar{S}}^a)^{-1}(\overline{\overline{Id}} + \bar{\bar{S}}^a). \tag{15}$$

We see that measurements of the scattering parameters at the measurement ports can be converted to the scattering parameters at the probe array network ports using Equation 14 and those scattering parameters can be converted to the probe array mutual impedance matrix using Equation 15.

5 Example Results from Numerical Analysis

We conclude with an elementary example consisting of a three element probe array. This example is included to demonstrate performance when the probe array element currents induced by the plane wave and body scattering are canceled by probe array element sources. The measure of performance is the error in the target dipole currents produced by the canceled probe element sources when compared to the free space currents induced when the probe array is absent.

As illustrated in Figure 13, the probe array consists of three dipoles of length 0.48λ and inter-element spacing of $\lambda/2$. Three surrogate target dipoles of length $\lambda/2$ are located 5λ away from the array as illustrated and one target dipole is 35λ from the probe array and offset by 5λ. The probe array and target dipoles are illuminated by a plane wave, initially broad side to the probe array and then 75^o from the broadside. Note that in this example the probe array elements are driven directly by voltage sources rather than via transmission lines.

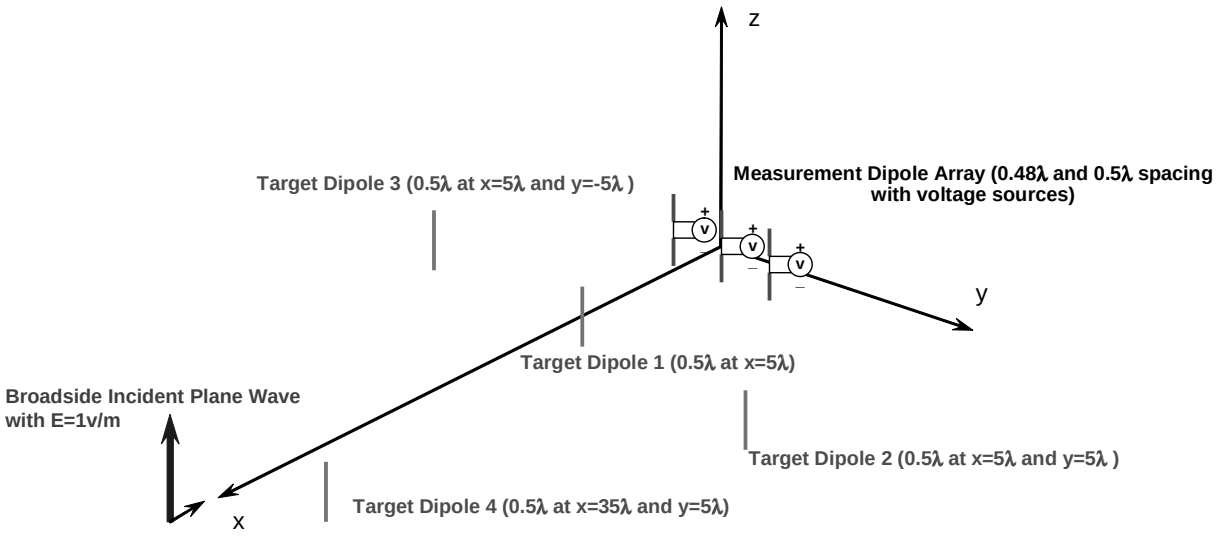

Figure 13: Geometry for Three Element Probe Array and Target Dipoles

Analysis of this configuration was performed using NEC4 to account for the electromagnetic interaction between probe array elements and the target dipoles as well as the in situ mutual impedances between the probe array elements. Initially the in situ mutual impedances are determined using NEC4 by driving each element separately with its voltage source and calculating the short-circuit current in the probe array elements, in effect determining the in situ admittance matrix of the array. The array mutual impedance matrix is the inverse of the admittance matrix. For these impedance calculations, no plane wave excitation is applied. Next the probe array element voltage sources are adjusted using the impedance matrix to cancel the currents induced in the probe array elements by the plane wave excitation. In this state, the currents in the target dipoles are calculated and compared with those induced by the plane wave alone without the probe array present.

Results of this analysis are shown in Figures 14 and 15 for broadside plane wave excitation and Figures 16 and 17 for plane wave excitation which is 75^o from broadside illumination. Figure 14 shows the currents in the short-circuited probe array elements when excited by the broadside plane wave and the currents in the probe array elements with the cancelation voltage applied. The currents on the end elements are identical because of symmetry and so only four curves are shown. It is clear that complete current cancelation occurs only at the port where the voltage is applied. Residual currents occur on the quarter wavelength ends of the probe element dipoles and these residual currents are approximately 20 dB below the currents on the short-circuit dipoles. It is clear once again that complete current cancelation with only a single load point is not possible leaving residual dipole currents that can reradiate and disturb the plane wave induced currents on the target dipoles.

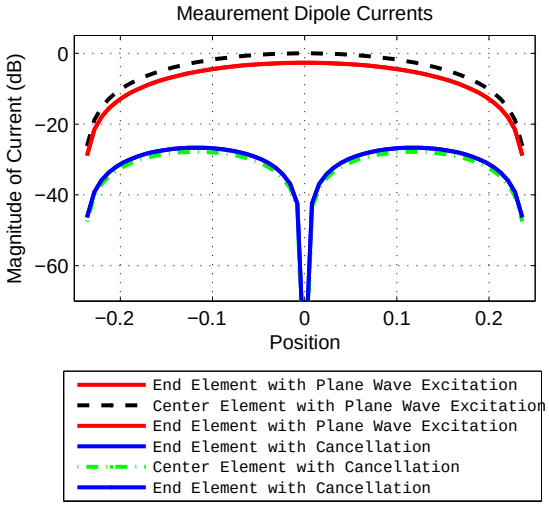

Figure 14: Short-Circuit and Canceled Currents on Probe Array Dipoles -Broadside Plane Wave Excitation

The target dipole currents are shown in Figure 15. The current distributions on each of the target dipoles shown in Figure 13 is plotted with the measurement array absent and with the canceled currents on the measurement array. The current distribution when the measurement array is absent is considered the reference since no perturbation of the plane wave induced currents is possible in this case. In Figure 15 it is impossible to distinguish differences between these current distributions and so we have plotted the magnitude of the difference in the complex currents in two cases. These are (1) the magnitude of the error between the plane wave induced currents with measurement array absent and with the short-circuited array present and (2) the magnitude of the error between the plane wave induced currents with the measurement array absent and with the canceled current array present. Figure 15 shows that canceling the probe currents reduces the error in the target dipole currents by 20 dB or more. The magnitude of the error in the induced currents with the probe array present and currents canceled is between -40 dB and -60 dB with respect to the free space, plane wave induced currents.

Figures 16 and 17 show similar results when the plane wave excitation is 75^o from broadside. Once again, the probe element currents are canceled well only at the load point leaving residual

currents to reradiate and modify the free space plane wave induced currents on the target dipoles (Figure 16). In Figure 17 we see that the errors introduced by the probe array with canceled currents are smaller by approximately 10 dB in the center, near-target dipole and far-target dipole when compared to the broadside illumination case. Also the errors in the displaced near-target dipoles (dipoles 2 and 3) are larger by 20 dB when compared to the broadside illumination but these errors are still below 40 dB when compared to the free space, plane wave induced currents.

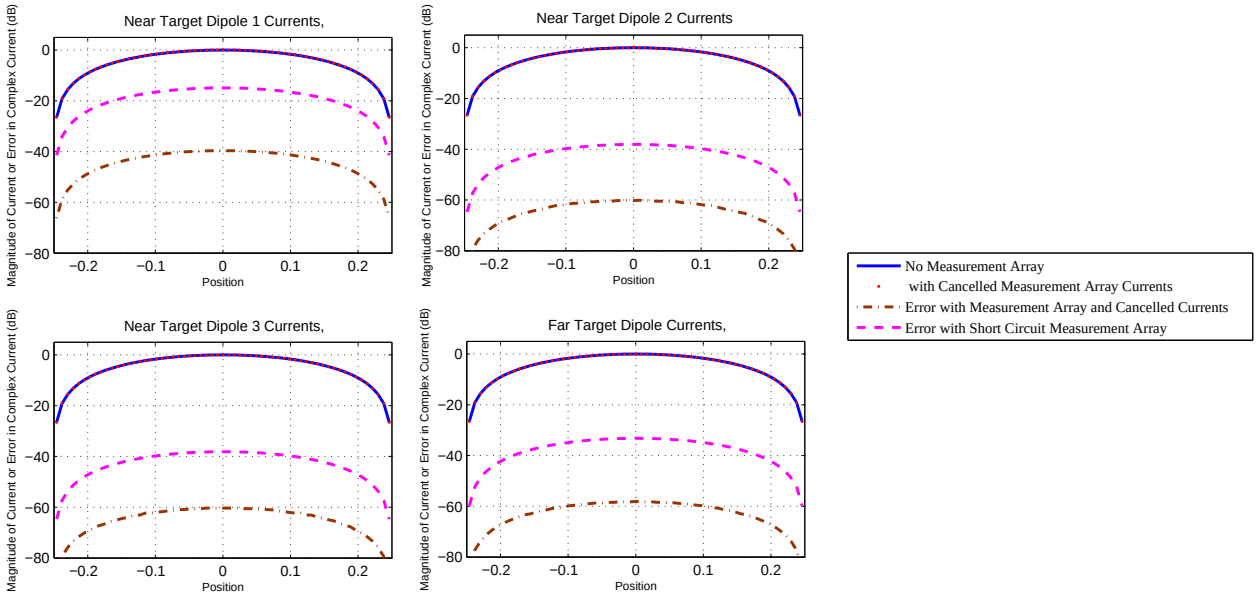

Figure 15: Currents on Target Dipoles and Errors when Compared to Short-Circuit and Canceled Current Measurement Array - Broadside Plane Wave Excitation

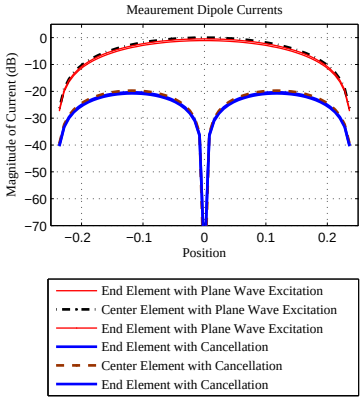

Figure 16: Short-Circuit and Canceled Currents on Probe Array Dipoles - Plane Wave Excitation at 75^o from Broadside

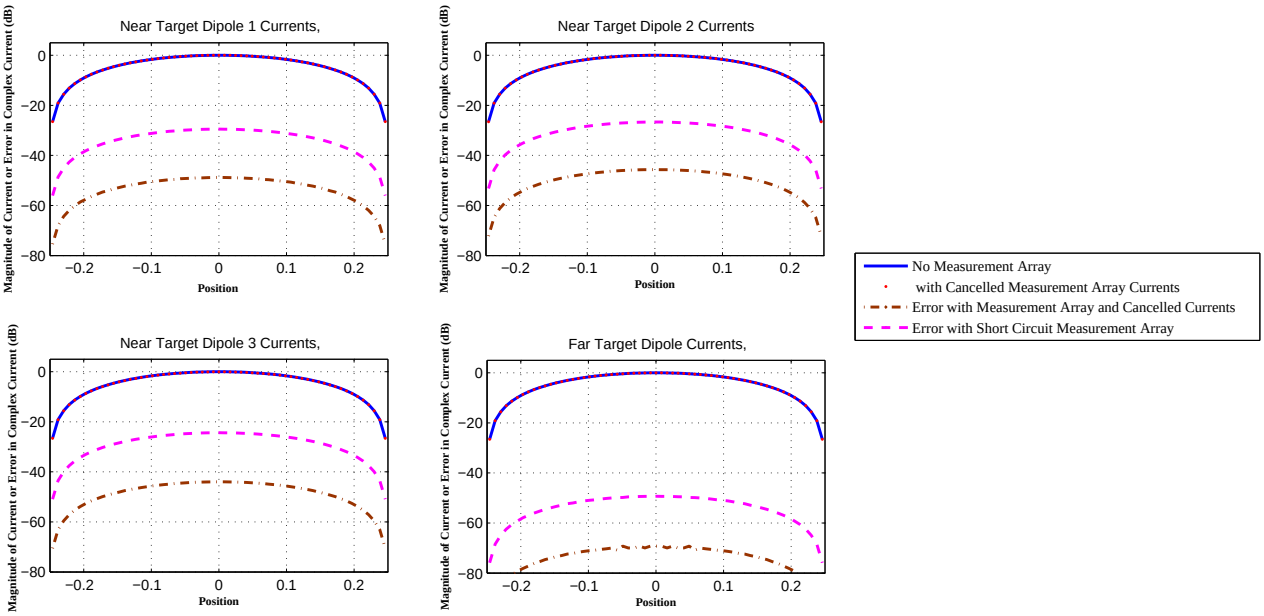

Figure 17: Currents on Target Dipoles and Errors when Compared to Short- Circuit and Canceled Current Measurement Array - Plane Wave Excitation at 75^o from Broadside

6 Conclusions and Recommendations

We have studied an active loading approach to minimize the electromagnetic interactions between an array of field probes and a nearby scattering body. The loading minimizes the currents on the array of field probes while simultaneously measuring the open-circuit voltages induced in the probes. We hypothesize that these open-circuit voltages, when corrected for the direct plane wave excitation, are proportional to the near-zone scattered field of the body at the probe locations. These near-zone field measurements are useful for efficiently synthesizing the far-zone bistatic scattering from the body.

Numerical studies of simple examples show that the currents on the approximately half wavelength probe array elements are canceled effectively only at the single load point, leaving residual currents to reradiate and modify the plane wave induced currents on the scattering body. Nevertheless, examination of the currents on surrogate target dipoles indicates that substantial reductions in the errors in the induced currents results from the single point loading of each element in a three element probe array.

A theory for the active loading was developed for a general case of the probe array fed by active loads through transmission lines to each element of the probe array. Measurement of the plane wave induced voltages at each of the load ports provides sufficient data to evaluate the plane wave induced open-circuit voltages at each of the probe array ports. We hypothesize that these open-circuit voltages, when corrected for the direct plane wave excitation, are proportional to the required near-field samples. However, inversion of the measured data requires additional

measurements of the in situ mutual and self impedances of the probe array. Here we use the terminology "in situ" to connote the requirement that the impedances be measured when the probe array in located near to the scattering body, and not in free space.

While the theory and simple numerical results are encouraging, further analysis is required of several issues. These are:

- Calibration of the open-circuit, plane wave-induced voltages. As indicated, we have hypothesized that the open-circuit voltages induced in the probe array elements by the plane wave and the scattering body, when corrected for the direct plane wave excitation, are proportional to the required near-field samples of the body scattering. This hypothesis needs to be investigated to insure that the voltages in the probe array elements are a close approximation to the voltages induced in a single probe dipole at the same location. Further, calibration of the probe array elements (an effective dipole length) needs to be developed to convert the open-circuit voltages to the corresponding electric field samples.

- Measurement of the in situ impedances of the probe array. The self and mutual impedances of the probe array are a function of the geometry of the probe array itself as well as the orientation of the array with respect to the nearby scattering body. Since the probe array will be moved with respect to the scattering body to accumulate the near-scattered field measurements, it may be necessary to measure the self and mutual impedances at each probe array position. Since these measurements will extend the overall measurement time and the objective of the probe array is to reduce this measurement time, we need to examine whether and how frequently the mutual impedance measurements must be made. For example, can we use the impedances measured in free space and still achieve sufficient accuracy in the induced, open-circuit voltages? If not, how often must the impedance measurements be updated as the probe array moves near the scattering body? With what precision do the impedances need to be measured?

- Experimental and/or numerical confirmation of the theory. An investigation of the active loading approach described here when used against realistic scattering bodies (and not the surrogate dipoles described here) needs to be conducted. Such an investigation could be conducted in an experimental facility or with numerical electromagnetic codes with the objective of comparing the measurements made with the probe array with those made using an isolated probe as is conventionally done in near-field bistatic scattering ranges. The investigation would provide confidence in the accuracy of the probe array approach and provide data to estimate processing requirements and time reductions implicit in the probe array approach for near-field bistatic measurements.

7 Acknowledgments

Support for this work from the Air Force Office of Scientific Research is gratefully acknowledged. Technical discussions with Dr. Kris Kim and Dr Hans Steyskal were important in developing the ideas described here. In addition, Dr. Kim suggested the problem and was instrumental in organizing the focused research program of which this is part. Dr. Steyskal pointed out the important requirement for correcting the measurements for direct plane wave excitation.

8 References

[1] Harrington, R. F., "Theory of Loaded Scatterers," Proceedings of IEE, Vol. 111, No. 4, April 1964.

[2] Orfanidis, S. J., Electromagnetic Waves and Antennas, pp 420 - 423, available at the following web site: www.ece.rutgers.edu/~orfanidi/ewa/.

[3] Ibid, pp 425 - 428.